Glucagon receptor-mediated regulation of gluconeogenic gene transcription is endocytosis-dependent in primary hepatocytes

Jan Mikhale B. Cajulao[a], Eduardo Hernandez[a], Mark E. von Zastrow[b], and Erica L. Sanchez[a,*]
[a]San Francisco State University, Department of Biology, San Francisco State University, San Francisco CA 94132;
[b]University of California San Francisco, Department of Psychiatry, University of California San Francisco, San Francisco CA 94122

ABSTRACT **A number of G protein-coupled receptors (GPCRs) are now thought to use endocytosis to promote cellular cAMP signaling that drives downstream transcription of cAMP-dependent genes. We tested if this is true for the glucagon receptor (GCGR), which mediates physiological regulation of hepatic glucose metabolism via cAMP signaling. We show that epitope-tagged GCGRs undergo clathrin- and dynamin-dependent endocytosis in HEK293 and Huh-7-Lunet cells after activation by glucagon within 5 min and transit via EEA1-marked endosomes shown previously to be sites of GPCR/Gs-stimulated production of cAMP. We further show that endocytosis potentiates cytoplasmic cAMP elevation produced by GCGR activation and promotes expression of phosphoenolpyruvate carboxykinase 1 (PCK1), the enzyme catalyzing the rate-limiting step in gluconeogenesis. We verify endocytosis-dependent induction of *PCK1* expression by endogenous GCGRs in primary hepatocytes and show similar control of two other gluconeogenic genes (*PGC1α* and *G6PC*). Together, these results implicate the endosomal signaling paradigm in metabolic regulation by glucagon.**

Monitoring Editor
JoAnn Trejo
University of California, San Diego

Received: Sep 10, 2021
Revised: May 26, 2022
Accepted: Jun 23, 2022

INTRODUCTION

G protein-coupled receptors (GPCRs) comprise the largest family of membrane proteins. GPCRs activate heterotrimeric G proteins in response to ligand-induced activation, then typically undergo regulated phosphorylation and bind to beta-arrestins. These events both attenuate GPCR-mediated activation of G proteins and promote receptor internalization. According to the classical view, GPCR signaling is restricted to the plasma membrane and internalized receptors are functionally inert (Harden *et al.*, 1980). An emerging revision to this classical paradigm is that GPCRs have the potential to also signal after endocytosis (Calebiro *et al.*, 2009; Irannejad *et al.*, 2013; Pavlos and Friedman, 2017; Stoeber *et al.*, 2018). Several GPCRs that initiate cAMP signaling through Gs (Rosenbaum *et al.*, 2009) have been shown to couple to Gs both from the plasma membrane and in endosomes. These Gs-coupled GPCRs use activation from endosomes to promote downstream signaling to the nucleus for control of cAMP-dependent gene expression (Irannejad *et al.*, 2013; Tsvetanova and von Zastrow, 2014; Peng *et al.*, 2021). The full physiological and biological effects of this second wave of cAMP generation are an area of active investigation.

Endocytosis has been shown to promote cAMP-dependent signaling to the nucleus and transcriptional control by Gs-coupled polypeptide hormone receptors (Tsvetanova and von Zastrow, 2014; Godbole *et al.*, 2017). For example, the thyroid stimulating hormone receptor must internalize for maximum transcription of genes that are part of the physiological response to thyroid stimulating hormone (Godbole *et al.*, 2017). In developing oocytes, the luteinizing hormone receptor internalizes to induce a second wave of cAMP signaling to the nucleus that promotes resumption of meiosis before ovulation (Lyga *et al.*, 2016). The degree to which endocytosis-dependent downstream signaling is initiated remains unknown

This article was published online ahead of print in MBoC in Press (http://www.molbiolcell.org/cgi/doi/10.1091/mbc.E21-09-0430) on June 29, 2022.

*Address correspondence to: Erica L. Sanchez, PhD (elsanchez09@sfsu.edu).

Abbreviations used: ANOVA, analysis of variance; B2AR, beta-2 adrenergic receptors; cAMP, cyclic adenosine monophosphate; CHC, clathrin heavy chain; DMSO, dimethyl sulfoxide; EDTA, ethylenediaminetetraacetic acid; EEA1, early endosome antigen 1; FACS, fluorescence activated cell sorting; G6PC, glucose-6-phosphatase; GAPDH, glyceraldehyde-3-phosphate dehydrogenase; GCGR, glucagon receptor; GPCR, G protein-coupled receptor; HEK293, human embryonic kidney 293; HPRT, hypoxanthine phosphoribosyltransferase; ISO, isoproterenol; PBS, phosphate buffered saline; PCC, Pearson's correlation coefficient; PCK1, phosphoenolpyruvate carboxykinase 1; PGC1α, peroxisome proliferator-activated receptor-gamma coactivator 1 alpha; RAMP2, receptor activity modifying protein 2; ROI, region of interest; SD, standard deviation; SEM, standard error of the mean; SIK1, salt-inducible kinase 1; SSF, signal sequence FLAG.

for other Gs-coupled polypeptide hormone receptors, such as the glucagon receptor (GCGR).

This study set out to explore whether endocytosis of GCGR was required for the transcriptional regulation of gluconeogenic gene expression. Blood glucose homeostasis is largely regulated by hormones, including insulin and glucagon, which have opposing physiological effects (Janah *et al.*, 2019). While insulin's effect is to reduce blood glucose during hyperglycemia, glucagon works to raise blood glucose levels during hypoglycemia (Janah *et al.*, 2019). Glucagon is a peptide hormone released by the alpha cells of the pancreas that acts on GCGR expressed in the liver to stimulate gluconeogenesis and raise blood glucose content (Janah *et al.*, 2019). A previous in vivo study found that a 5-d siRNA inhibition of endocytosis in mouse livers resulted in a loss in hypoglycemic homeostasis and a reduction of gluconeogenic gene transcription (Zeigerer *et al.*, 2015). However, the role of GCGR endocytosis was unexplored. Therefore GCGR is a GPCR whose subcellular signaling mechanisms have not yet been fully elucidated. Understanding the mechanisms and nuances of GCGR signaling could yield valuable insight for the receptor's pharmacology and treatment of various metabolism-related diseases (Campbell and Drucker, 2015; Janah *et al.*, 2019).

We hypothesized that the endocytosis of the GCGR is required for transcriptional regulation of key gluconeogenic target genes. This study confirmed that GCGR localizes to early endosomes upon stimulation and also demonstrated that endocytosis is required to elicit maximal cAMP production and expression of the gluconeogenic enzyme phosphoenolpyruvate carboxykinase 1 (PCK1). Moreover, GCGR endocytosis is required for maximal GCGR-dependent transcription of gluconeogenic genes in primary hepatocytes. Our results reveal a new and previously unappreciated understanding of GCGR subcellular signaling.

RESULTS

Stimulated GCGR translocates to endosomes

Several GPCRs signal at the cell surface, as well as within various intracellular locations after agonist stimulation. We hypothesized that upon stimulation with the glucagon peptide, that GCGR also traffics to the endosome. We first interrogated the trafficking and intracellular localization of GCGR after agonist stimulation. For these experiments, HEK293 cells were transiently transfected with the GCGR-MycDDK expression plasmid. GCGR and endosomal localization were visualized using antibody staining and confocal microscopy. Confocal images show GCGR primarily localizes to the plasma membrane in unstimulated cells (Figure 1, A and B). Quantification of these images by line scan analysis show intensity peaks at the ends of the lines that correspond to the cell surface (Figure 1, A and B, yellow arrowheads). When stimulated with glucagon, confocal images show that cytoplasmic GCGR increases and accumulates in early endosomes. Line scan analysis showed that cytoplasmic GCGR intensities increase and create noticeable peaks that correlate with peak intensities of the endosomal marker EEA1 (Figure 1, A and B, black arrowheads). To confirm that GCGR internalizes via the endocytosis mechanism, we first treated cells with Dyngo, a drug inhibitor that targets Dynamin (Figure 1A). We also performed these experiments upon siRNA knockdown of clathrin heavy chain (CHC17), a gene critical for endocytosis (Figure 1B). Upon treatment with glucagon, cells pretreated with Dyngo failed to accumulate GCGR at endosomes. Similarly, GCGR did not accumulate at endosomes in cells where clathrin was knocked down. These are highlighted by the lack of intracellular GCGR puncta and intensities that correlate with EEA1 (Figure 1B).

GCGR and endosomal localization was further analyzed by calculating Pearson's Correlation Coefficient (PCC) for GCGR and EEA1 (Figure 1C). GCGR colocalized with the endosomal marker EEA1 upon stimulation with glucagon. Inhibition of endocytosis, via treatment with 30 μM Dyngo, prevented GCGR from trafficking to the endosomes after glucagon stimulation. No significant differences were found by PCC when comparing unstimulated control cells with glucagon-stimulated samples with either Dyngo or siCHC17 treatment. Knockdown of CHC17 was confirmed with qPCR and Western blot (Figure 1, D and E).

Finally, we performed surface-labeling assays to confirm internalization of GCGR. For these experiments, we treated HEK293 cells stably expressing SSF-GCGR with or without glucagon for 30 min. We then labeled the plasma membrane-localized GCGR using the M1 Flag antibody followed by FACS analysis (Figure 1F). Indeed, less surface-labeled GCGR was detected in cells treated with glucagon, as measured by a significant reduction in mean GCGR fluorescence intensity. This confirms that GCGR internalizes upon stimulation. Together, line scan, colocalization, and FACS analyses indicate that GCGR, upon stimulation with glucagon, internalizes and traffics via endocytosis.

We then examined GCGR trafficking in a hepatocyte cell line, Huh-7-Lunet. Stable Huh-7-Lunet cells expressing SSF-GGCR were pretreated with DMSO or Dyngo-4a and then treated with or without 1 μM glucagon for 30 min. As with the HEK293 cells, GCGR and endosomal localization were visualized using antibody staining and confocal microscopy (Figure 2A). In addition to surface localization of SSF-GCGR, some intracellular receptor was detected in unstimulated samples. Line scan analysis shows GCGR intensity peaks at the ends of lines corresponding to surface-localized receptor in all samples (yellow arrowheads) and GCGR peaks that correlate with EEA1 peaks (black arrowheads). Stimulation with glucagon leads to more GCGR peaks that correlate with EEA1 peaks in DMSO-treated samples but not samples with endocytic blockade.

Further image analysis shows that colocalization between GCGR and EEA1 was highest in glucagon-stimulated cells without endocytic blockade (Figure 2B). Together, these images indicate that GCGR localizes to endosomes upon stimulation with glucagon in a hepatocyte cell line.

GCGR endocytosis occurs within 5 min of stimulation

We then investigated the time dependency of GCGR endocytosis. Cells were stimulated with glucagon over time from 0 to 30 min. GCGR and EEA1 colocalization was visualized using confocal microscopy (Figure 3A). Images show that SSF-GCGR is primarily localized to the plasma membrane in HEK293 cells before stimulation and colocalizes with EEA1 within 5 min of glucagon treatment. In Huh-7-Lunet cells, some GCGR is detected in the cytoplasm prior to stimulation. After further analysis via PCC calculation, significant colocalization is observed within 5 min of glucagon treatment and reaches a maximum after 10 min in both cell lines (Figure 3B).

Endocytosis modulates GCGR signal transduction

After determining that GCGR traffics via endosomes in response to stimulation with glucagon, we sought to determine the requirement of endocytosis on GCGR-dependent signaling and downstream transcriptional regulation. Several GPCRs depend on endocytosis to achieve maximal transcriptional regulation, including the beta 2 adrenergic receptor (B2AR) (Irannejad *et al.*, 2013). In previous work, it was determined that B2AR, an endogenously expressed GPCR in HEK293 cells, signals in an endocytosis-dependent manner (Tsvetanova and von Zastrow, 2014). Additionally, the gluconeogenic enzyme PCK1 was identified as an endocytosis-dependent transcriptional target of B2AR. For this study, we hypothesized that

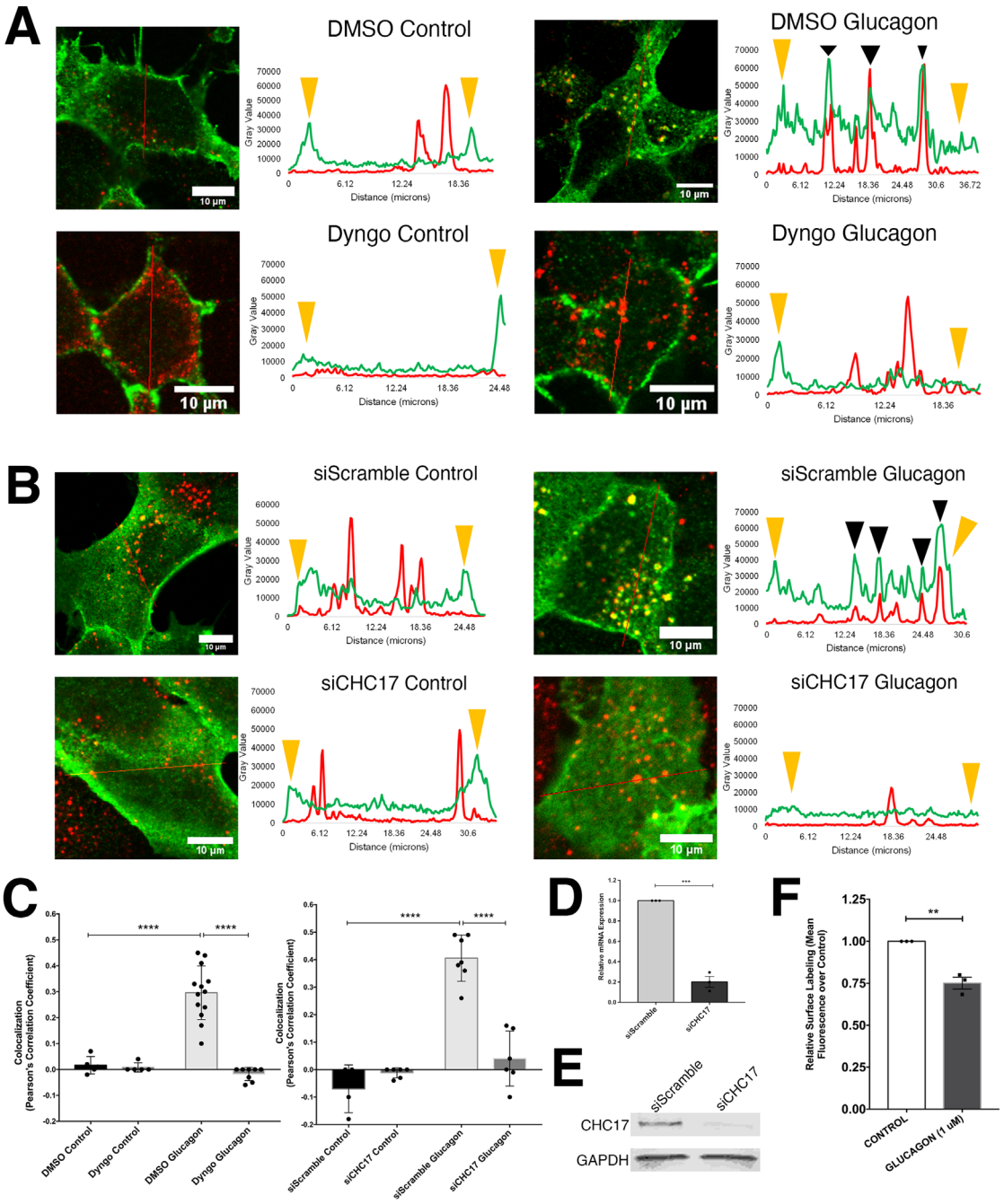

FIGURE 1: GCGR internalizes and localizes to endosomes upon stimulation with glucagon. HEK293 cells transiently transfected with GCGR-MycDDK were treated with or without 1 µM glucagon for 30 min and analyzed by microscopy or flow cytometry. (A, B) Line scan analysis was performed on confocal microscopy images of cells labeled for GCGR (green) and EEA1 (red). Endocytosis was inhibited by either (A) pretreatment for 15 min with or without 30 µM Dyngo or (B) transfection with siCHC17, or with siScramble as a control. GCGR localizes to the plasma membrane (yellow arrowheads) but translocates to endosomes upon stimulation (black arrowheads). Endocytic blockade via drug or siRNA prevented GCGR accumulation in endosomes. (C) Colocalization of GCGR and EEA1. Pixel intensities from confocal microscopy images were analyzed with the ImageJ Coloc 2 plugin. Left: cells were pretreated for 15 min with or without 30 µM Dyngo to block endocytosis. Right: cells were transfected with siCHC17, or with siScramble as a control. GCGR colocalized with EEA1 after stimulation unless endocytosis was inhibited. All data are mean ± SD. Significance determined by ordinary one-way ANOVA followed by Tukey's multiple comparisons test (****p value < 0.0001) (D, E) CHC17 knockdown validation in siRNA-transfected HEK293 cells. (D) qPCR analysis of *CHC17* mRNA expression in siCHC17 or Scrambled siRNA-transfected cells. (E) Western blot analysis of CHC17 expression in siCHC17 or Scrambled siRNA-transfected cells. (F) Upon 30-min treatment with 1 µM glucagon, HEK293 cells stably expressing SSF-GCGR were labeled with M1 Flag antibody conjugated to Alexa Fluor 647, fixed, and prepared for flow cytometry. Surface labeling of GCGR was measured. Mean fluorescence from three independent experiments were normalized to unstimulated control cells. All data are mean ± SEM. Significance determined by unpaired two-tailed *t* test. (**p value < 0.05).

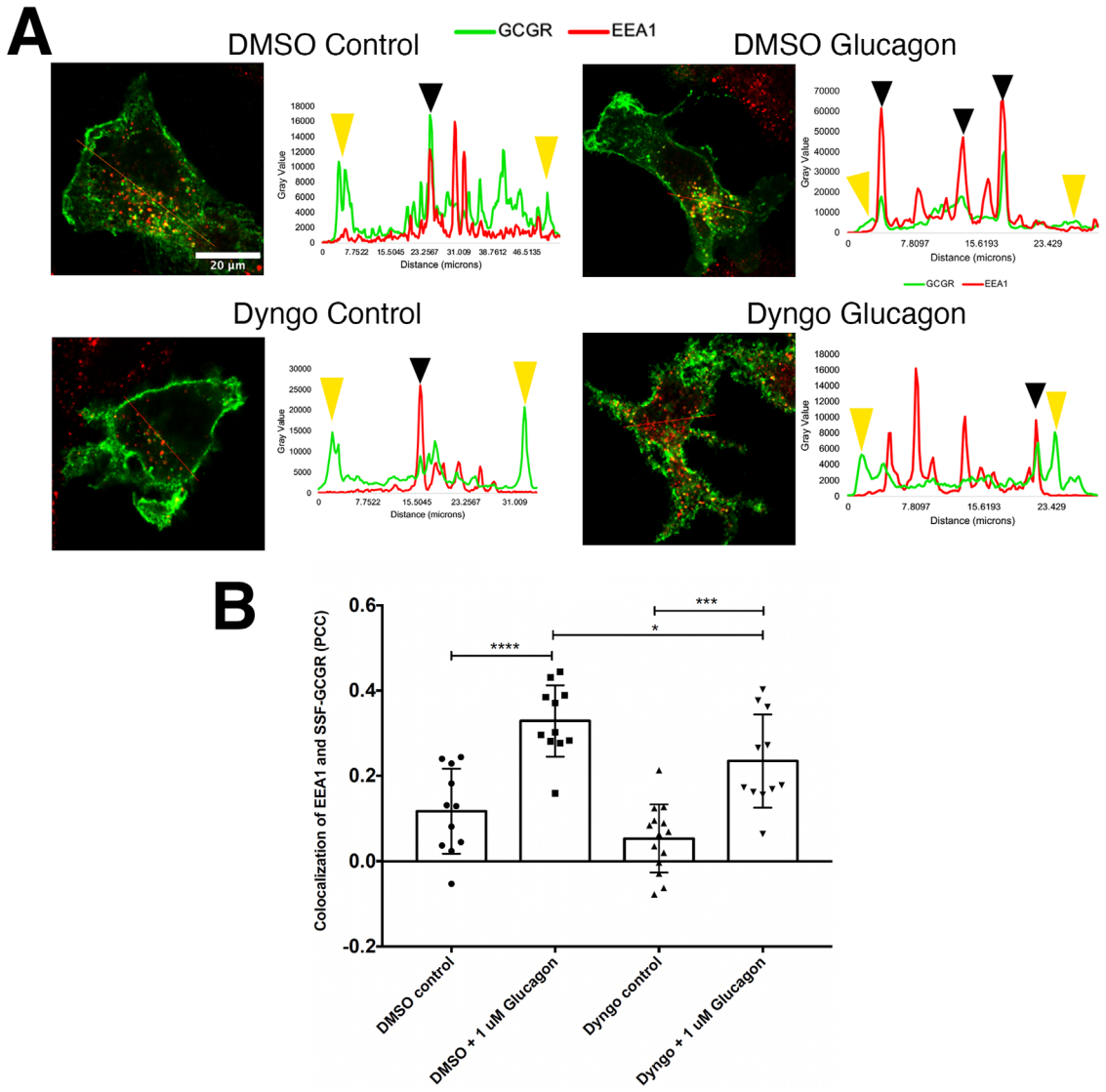

FIGURE 2: GCGR internalizes and localizes to endosomes upon stimulation with glucagon in Huh-7-Lunet cells. Huh-7-Lunet cells stably expressing SSF-GCGR pretreated with or without Dyngo-4a were then treated with or without 1 µM glucagon for 30 min and imaged via confocal microscopy. (A) Confocal microscopy images and line scan analyses of control or glucagon-stimulated Huh-7-Lunet-SSF-GGCR cells pretreated with DMSO or Dyngo-4a to block endocytosis and labeled for GCGR (green) and the early endosome marker EEA1 (red). Intensity plot profiles corresponding to red line drawn on images are shown. Green and red lines on plots correspond to GCGR and EEA1 intensities, respectively, and are annotated to highlight surface-localized GCGR (yellow arrowheads) and endosome-localized GCGR (black arrowheads). (B) Bar plots of mean GCGR and EEA1 colocalization. Pixel intensities from confocal microscopy images were analyzed with EzColocalization, and PCC was calculated. GCGR colocalized with EEA1 after stimulation, and colocalization was reduced by Dyngo-4a pretreatment. Dots represent individual cells. Data are mean ± SD. Significance was determined by two-way unpaired *t* test (*$p < 0.05$, ***$p < 0.001$, ****$p < 0.0001$).

this gluconeogenic target is also regulated by endocytosis-dependent GCGR-signaling. Both GCGR and B2AR signal via the Gs subunit and generate cAMP as a second messenger. Therefore we included B2AR stimulation in our experiments as an internal positive control to verify that cAMP is produced in response to agonist stimulation and that endocytic blockade inhibits Gs-mediated cAMP production.

To investigate whether GCGR signaling is endocytosis dependent, we measured the production of cAMP and expression of *PCK1* in the presence or absence of endocytosis inhibition with Dyngo. Using a pGLO-based cAMP biosensor, we measured cAMP production over time in cells after treatment with glucagon or isoproterenol in the presence or absence of Dyngo pretreatment. Both isoproterenol and glucagon stimulated cells resulted in prominent cAMP production compared with untreated cells. For both isoproterenol- and glucagon-stimulated cells, relative luminescence over time was reduced in cells that were pretreated with Dyngo. Further analysis revealed that peak cAMP intensities in glucagon- and isoproterenol-stimulated cells were significantly higher than cells pretreated with Dyngo (Figure 4, A and B).

As previously published for B2AR stimulated cells, PCK1 transcription was significantly induced by glucagon stimulation unless cells were pretreated with Dyngo to inhibit endocytosis (Figure 4C). HEK293 cells stably expressing SSF-GCGR stimulated with glucagon show a significant up-regulation of *PCK1* transcription; however, this up-regulation is inhibited by endocytic blockade. A 23.4-fold

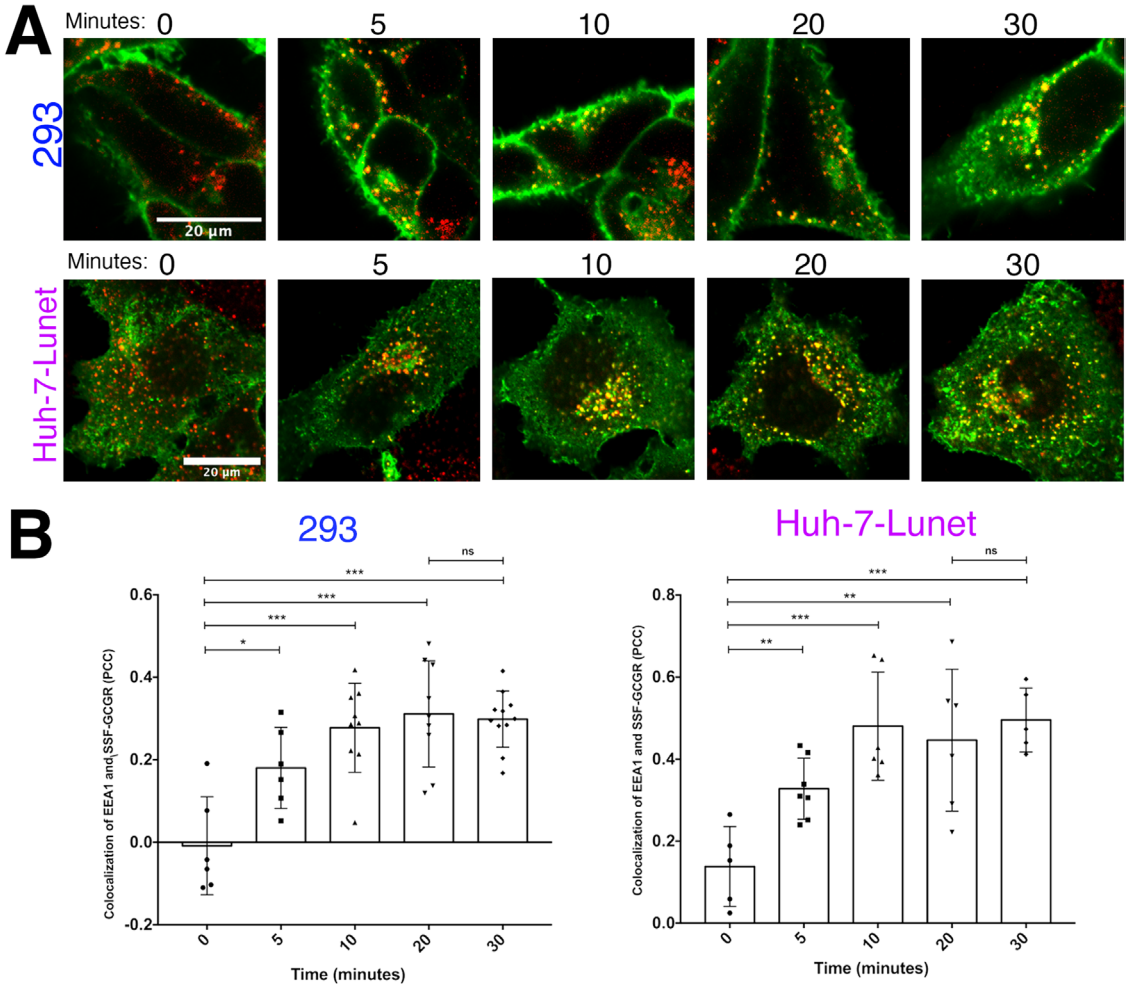

FIGURE 3: Endosomal localization of GCGR occurs within 5 min in HEK293 and Huh-7-Lunet cells. Cells stably expressing SSF-GCGR were treated with 1 µM glucagon for 0 to 30 min. GCGR (green) and EEA1 (red) were labeled and samples were analyzed with confocal microscopy. (A) Confocal microscopy images of cells at each time point. (B) Bar plots of GCGR and EEA1 colocalization over time, as measured by PCC. Confocal microscopy images were analyzed by the ImageJ plugin EzColocalization to calculate PCC of each cell. Dots represent individual cells, and bars represent mean ± SD. Significance was determined by *t* test (ns, not significant; $*p < 0.05$, $**p < 0.01$, $***p < 0.001$).

glucagon-dependent *PCK1* up-regulation in DMSO pretreated cells was observed compared with a 12.6-fold up-regulation in Dyngo pretreated cells.

As mentioned earlier, B2AR, a GPCR coupled to Gs, signals in an endocytosis-dependent manner. A previously published screen revealed endocytosis-dependent transcriptional targets of the cAMP-stimulating B2AR (Tsvetanova and von Zastrow, 2014). This screen also identified targets that were up-regulated by stimulated B2AR but whose up-regulation was not attenuated by endocytic blockade, including salt-inducible kinase 1 (*SIK1*). For this study we were interested if all glucagon-dependent genes were also endocytosis dependent and therefore examined *SIK1* transcription in addition to *PCK1*. We show that glucagon does indeed up-regulate *SIK1* in HEK293 cells stably expressing SSF-GCGR, and that this up-regulation is not attenuated by endocytic blockade. No statistically significant difference in *SIK1* transcription was found between glucagon-stimulated DMSO or Dyngo pretreated cells ($p = 0.90$, $n = 3$) (Figure 4C)

We further examined how endocytosis regulates protein expression of PCK1 in HEK293 cells stably expressing SSF-GCGR. Cells were stimulated with 1 µM glucagon for up to 4 h with or without endocytic blockade. Western blot analysis showed that PCK1 expression is up-regulated by glucagon after 2 and 4 h. Furthermore, Dyngo-4a-pretreated cells show reduced glucagon-dependent transcription of PCK1 after 2 and 4 h of glucagon stimulation (Figure 4D). Together, these data indicate that the generation of maximal cAMP and expression of *PCK1* are dependent on the endocytosis of GCGR.

Endocytosis is required for maximal GCGR-dependent transcriptional regulation in primary mouse hepatocytes

GCGR is endogenously expressed in the liver and serves as a regulator of blood glucose by up-regulating gluconeogenic genes during hypoglycemic conditions (Janah *et al.*, 2019). We sought to confirm that GCGR requires endocytosis for maximum transcription of gluconeogenic genes in a biologically relevant cell type. For this, experiments were conducted using primary mouse hepatocytes obtained from the UCSF Liver Center. Immediately following harvest, hepatocytes were seeded onto collagen-coated cell culture plates. Twenty-four hours after plating, cells were pretreated with or without Dyngo and then treated with 100 nM glucagon for 2 h. RNA was harvested for gene expression analysis by qRT-PCR. Gene expression was determined for the gluconeogenic genes, *PCK1*, glucose-6-phosphatase

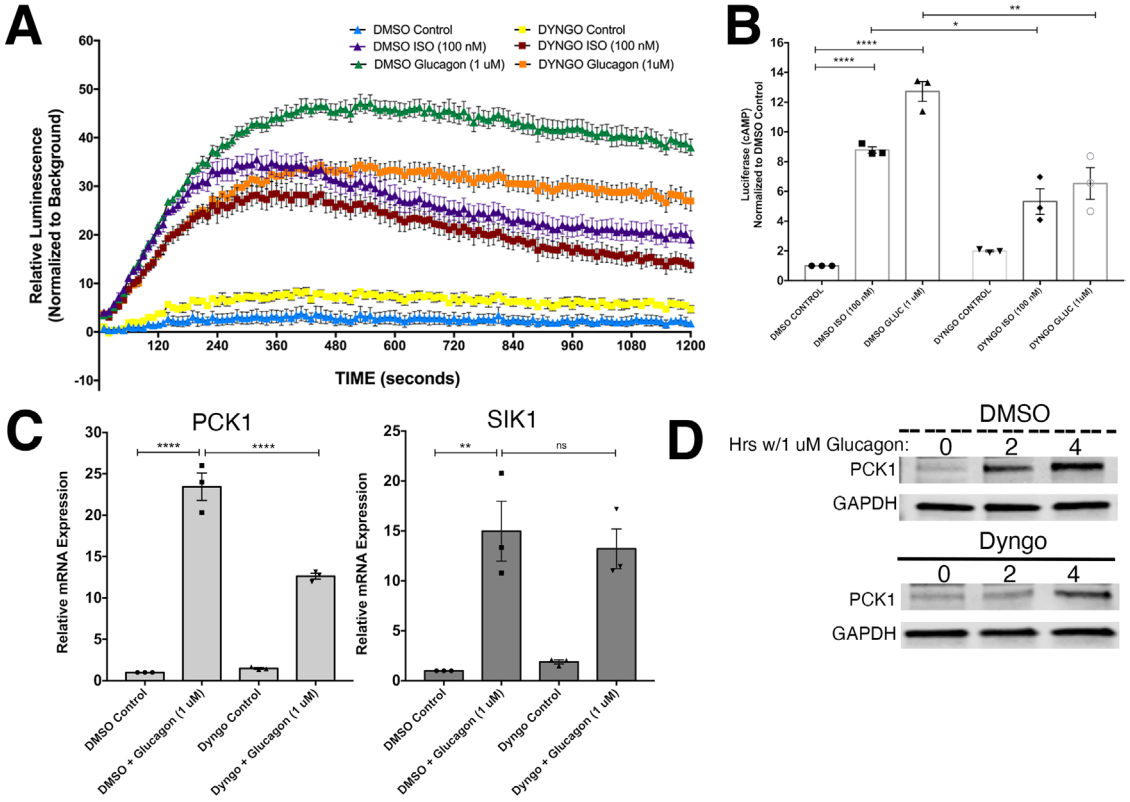

FIGURE 4: Maximal GCGR signaling is endocytosis dependent. (A) HEK293 cells stably expressing SSF-GCGR were transfected with pGLO cAMP Biosensor. Cells were then pretreated with or without 30 μM Dyngo. Upon treatment with or without 100 nM Isoproterenol or 1 μM glucagon, luminescence was measured every 10 s for 20 min. Representative data from one of three biological replicate experiments are shown. (B) Average peak intensities normalized to DMSO Control luminescence. (C) HEK293 cells stably expressing SSF-GCGR were pretreated with or without 30 μM Dyngo to block endocytosis. Cells were then treated with or without 1 μM glucagon. qPCR was used to quantify relative mRNA levels of PCK1 and SIK1. Endocytic blockade inhibits GCGR-dependent transcription of PCK1 but not SIK1. All data are mean ± SEM. Statistical significance calculated by ordinary one-way ANOVA with multiple comparisons using a Tukey test. $^{**}p < 0.01$, $^{****}p < 0.0001$. Statistical comparison between DMSO Control and Dyngo Control are not significant. (D) Western blot analysis of endocytosis- and glucagon-dependent PCK1 expression. HEK293-SSF-GCGR cells were pretreated with DMSO or Dyngo-4a to block endocytosis for 15 min, followed by 2 to 4 h of stimulation with 1 μM glucagon. Protein was harvested from cells and analyzed via Western blot. Dyngo pretreated cells stimulated with 1 μM glucagon show reduced capacity for glucagon-dependent PCK1 expression.

(*G6PC*), and peroxisome proliferator-activated receptor-gamma co-activator 1 alpha (*PGC1α*) in response to glucagon stimulation and inhibition of endocytosis. Gene expression of all three gluconeogenic targets was highly induced by glucagon stimulation; however, this up-regulation was attenuated upon endocytic inhibition (Figure 5). Our data suggest that the transcription of gluconeogenic genes is endocytosis dependent in primary hepatocytes.

DISCUSSION

Several studies have found that GPCR signaling after endocytosis is critical for maximal downstream regulation of transcription (Irannejad *et al.*, 2013; Tsvetanova and von Zastrow, 2014; Tsvetanova *et al.*, 2015; Pavlos and Friedman, 2017). The findings from our study demonstrate that upon activation by glucagon, GCGR must internalize for maximum transcription of gluconeogenic genes (Figure 6).

First, we determined that upon ligand-dependent internalization, GCGR localizes with endosomes in HEK293 cells (Figure 1) and the liver cell line Huh-7-Lunet (Figure 2). Endosomal localization occurs within 5 min of stimulation (Figure 3) and is required for maximum GCGR signaling as measured by cAMP production and up-regulation of PCK1 in HEK293 cells (Figure 4). We then confirmed the importance of endocytosis in primary mouse hepatocytes, where we found that endocytosis is required for glucagon-dependent up-regulation of PCK1, PGC1α, and G6PC (Figure 5). Together, our results support the notion that upon stimulation with glucagon, GCGR internalizes and localizes to the endosomes, and that this localization is required to exert maximal up-regulation of gluconeogenic genes (Figure 6).

The effect of endocytosis on GCGR signaling is seen within minutes at the second messenger level (Figure 4, A and B) but is also observed over a longer period as measured by PCK1 expression. Western blots show PCK1 expression is reduced due to endocytic blockade with 2 and 4 h of glucagon stimulation (Figure 4, C and D), suggesting that the contribution of internalized GCGR becomes apparent within minutes and persists for up to 4 h.

Receptor activity modifying protein (RAMP) 2 has been shown previously to modify trafficking and signaling of GCGR (Cegla *et al.*, 2017; McGlone *et al.*, 2021). Previous studies in HEK293 cells showed RAMP expression is low and not sufficient for modulation of GCGR activity (Bouschet *et al.*, 2005; Weston *et al.*, 2015). Therefore HEK293 overexpressing SSF-GCGR offer a cell line to study endocytic trafficking of GCGR without the effects of signaling background from endogenous GCGR, nor trafficking interference from endogenous RAMPs. Our data show that GCGR endocytosis occurs in both HEK293 and Huh-7-Lunet cells. Interestingly,

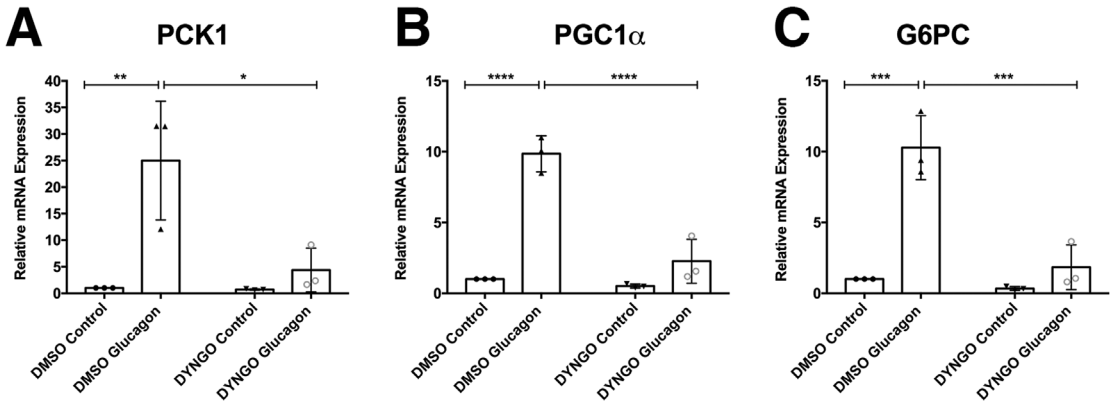

FIGURE 5: Endocytosis is required for maximal GCGR-dependent gluconeogenic gene transcription in primary mouse hepatocytes. Primary mouse hepatocytes were pretreated or with or without 30 μM Dyngo for 15 min to block endocytosis before subsequent treatment with or without 100 nM of glucagon for 2 h. Relative mRNA expression was measured by qRT-PCR for gluconeogenic genes (A) PCK1, (B) PGC1α, and (C) G6PC; $n = 3$ replicate plates of primary hepatocytes, two plates from one independent hepatocyte harvest and one plate from another independent hepatocyte harvest. Statistical significance calculated by ordinary one-way ANOVA with multiple comparisons using a Tukey test. *$p < 0.05$, **$p < 0.01$, ***$p < 0.001$. For all targets (A–C), statistical comparison between DMSO Control and Dyngo Control as well as Dyngo Control and Dyngo glucagon are not significant. Error bars represent mean ± SD.

more internalized GCGR was found in unstimulated Huh-7-Lunet cells than in unstimulated HEK293 cells (Figure 3). We hypothesize that this is due to the Huh-7-Lunet cell line expressing RAMP2 (Weston *et al.*, 2015) shown previously to promote internalization and endocytic localization of GCGR (Cegla *et al.*, 2017; McGlone *et al.*, 2021).

Future experiments could confirm the requirement of RAMP-2 or Beta Arrestin by inhibiting either mechanism and interrogating gluconeogenic gene transcription after glucagon stimulation. Other studies have explored GCGR internalization mechanisms. Previous work found that internalization in hepatocytes may not be mediated by beta arrestin (Merlen *et al.*, 2006; Krilov *et al.*, 2008).

Subsequent studies should also explore the signaling activity of GCGR at the endosomal membrane, possibly using conformational biosensors, called nanobodies, specifically designed to bind activated GCGR. Nanobodies have been used to directly show that endosome-localized B2AR is in an active conformation (Irannejad *et al.*, 2013). Moreover, GCGR may localize to additional intracellular compartments other than the endosomes. Therefore we cannot rule out the possibility of cAMP generation from other membranes, as reported for the thyroid-stimulating hormone receptor (Godbole *et al.*, 2017). Determining specific mechanisms of subcellular GCGR signaling could inform future studies that explore new drug candidates in treating metabolic dysregulation.

Glucagon and GCGR play important roles in blood glucose homeostasis and are an attractive target for therapeutic intervention in metabolism (Bagger *et al.*, 2011). Despite this, the specific mechanisms of GCGR signaling have yet to be fully explored, particularly in the nuances of its subcellular signaling. These results highlight a key step between receptor activation and gluconeogenesis and support the biological relevance of subcellular GCGR signaling. Together, our findings demonstrate an important molecular step in the physiological response to hypoglycemia.

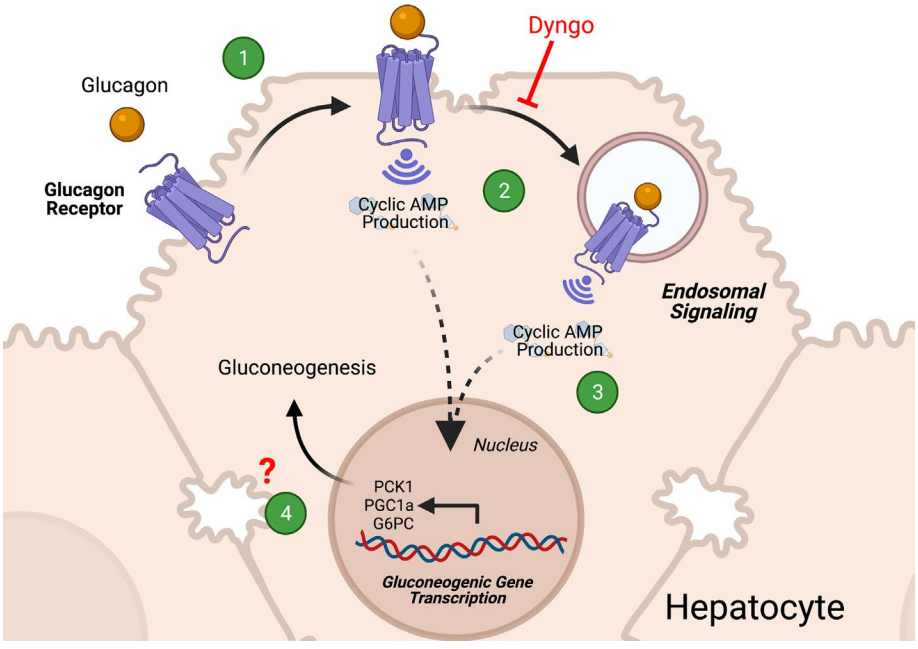

FIGURE 6: Model of endosomal GCGR signaling and gluconeogenic gene regulation. (1) The peptide hormone glucagon binds to the GCGR, which is expressed in the plasma membrane of hepatocytes. This initial binding triggers cAMP generation at the plasma membrane. (2) GCGR is internalized via endocytosis. (3) Our data show that after endocytosis, GCGR also generates a significant amount of cAMP. (4) Endocytic-GCGR signaling is required for maximal transcription of gluconeogenic genes in hepatocytes.

MATERIALS AND METHODS

Request a protocol through *Bio-protocol*.

Cell culture, expression constructs, and transfections

Human embryonic kidney 293 (HEK293) (ATCC CRL-1573) and Huh-7-Lunet cells were cultured in complete growth DMEM (Life Technologies) supplemented with 10% fetal bovine serum (UCSF Cell Culture Facility). Cells were passaged using trypsin or phosphate-buffered saline (PBS)-EDTA and maintained at 37°C and 5% CO_2. Transfections were performed using Lipofectamine 2000 (Life Technologies) according to the manufacturer's protocol. Cells were transfected 48 h before experiments. Primary cultures of mouse hepatocytes from male C57BL/6J mice were a generous gift from the UCSF Liver Center. Immediately following isolation, hepatocytes were plated on collagen-coated cell culture plates and grown for no longer than 48 h for all experiments (Corning BioCoat Collagen I, Cellware 6-well plate 356400). Hepatocytes were grown in DMEM supplemented with 10% fetal bovine serum and 1% penicillin-streptomycin (UCSF Cell Culture Facility). Microscopy experiments utilized the pCMV6-GCGR-MycDDK expression construct (OriGene Technologies, MR207767) or the generated signal sequence Flag-tagged GCGR, pcDNA3.1(+)_SSF-GCGR. All subsequent experiments used pcDNA3.1(+)_SSF-GCGR. Stable cell lines were generated and maintained by drug selection with Geneticin Selective Antibiotic, G418 (Life Technologies, Cat# 10131035).

Drug treatment and siRNA

The highly potent dynamin inhibitor, Dyngo-4A (Abcam, ab120689), was added 15 min prior to agonist treatment at a final concentration of 30 µM from a 30 mM stock dissolved in DMSO. Vehicle control was prepared by adding DMSO without Dyngo-4A. For siRNA transfections, cells were seeded at 50% confluency in a 10 cm dish and transfected with 200 pmol siRNA (Qiagen, Germantown, MD) using RNAiMax Lipofectamine (Life Technologies, Invitrogen) according to the manufacturer's protocol. Media were changed 24 h post-siRNA transfection and cells recovered for an additional 24 h before experimentation. For siRNA control samples, cells were transfected with All Star Negative (siScramble) SI03650318 and for knockdown of CHC (siCHC17) 5′-AAGCAATGAGCTGTTTGAAGA-3′.

Antibodies

Antibodies used were rabbit anti-Flag (Sigma), mouse anti-Flag M1 (Sigma), mouse anti-EEA1 (BD Biosciences), and rabbit anti-EEA1 (Invitrogen). Mouse anti-Flag M1 was conjugated to Alexa Fluor 647 for use in flow cytometry.

Fixed cell confocal imaging

Cells for experiments were either transiently transfected with indicated construct(s) and processed 48 h later or stable expression cell lines selected with G418. Cells seeded on glass coverslips (Fisher, 12-545-100) in 12-well plates were treated with or without Dyngo-4a followed by treatment with or without glucagon. After ligand treatment, cells were 1) rinsed with PBS, 2) fixed by incubation in 3.7% formaldehyde (Fisher Scientific) diluted in PBS buffer for 20 min at room temperature, 3) blocked in 2% bovine serum albumin (Sigma) in PBS with permeabilization by 0.2% Triton X-100 (Sigma), and 4) labeled by the addition of primary antibodies diluted in blocking/permeabilization buffer for 1 h; 5) secondary labeling was performed by the addition of the following antibodies diluted in blocking/ permeabilization buffer for 30 min at room temperature: Alexa Fluor 647 or 488 donkey anti-mouse (Invitrogen), Alexa Fluor 647 or 488 donkey anti-rabbit (Invitrogen). Specimens were mounted using ProLong Gold antifade reagent (Life Technologies).

Microscope image acquisition and image analysis

Fixed cells were imaged by spinning disk confocal microscope (Nikon Ti Inverted microscope with Yokogawa confocal scanner unit CSU22) using a 60× objective or a Zeiss LSM 710 mounted on a Zeiss Axiovert Imager.Z2 using a 63× objective. Fluorescence intensities were quantified and analyzed using the computer program ImageJ (https://imagej.nih.gov/ij/). Images were saved as uncompressed 16-bit TIFF images, then loaded into ImageJ. Line scan analysis measured intensities along a manually drawn line across a cell plotted using the Plot Profile function on ImageJ. Data were exported to Microsoft Excel and plotted on line graphs. Lines were drawn such that they intercepted endosomes and ran across the length of the cell. To quantify endocytosis of the GCGR, colocalization was analyzed using EzColocalization ImageJ package (Stauffer *et al.*, 2018). Cell outlines were manually drawn, and PCC between indicated channels was calculated. Mean PCC between samples was calculated and tested for statistical significance using a two tailed unpaired *t* test (GraphPad Prism).

Flow cytometry

HEK293 cells stably expressing pcDNA3.1(+)_SSF-GCGR were treated with or without 1 µM glucagon for 30 min at 37°C. Cells were then washed with PBS and fixed with 4% formaldehyde. Cells were incubated with Alexa Fluor 647–conjugated (Invitrogen, A20173) M1 mouse anti Flag monoclonal (Sigma, F-3040) antibody at 4°C for 1 h on a shaker. Cells were mechanically lifted and mean fluorescence intensity of 10,000 cells was measured by flow cytometry for each sample on a FACSCalibur (BD Biosciences). Internalization was calculated as the mean fluorescence intensity normalized to control samples. Each condition had three technical replicates per biological replicate.

cAMP luminescence assay

HEK293 stably expressing pcDNA3.1(+)_SSF-GCGR cells transfected with GloSensor20F (Promega) were lifted and resuspended in imaging media (DMEM without phenol red supplemented with 30 mM HEPES; Life Technologies, 31053 and 15640, respectively). Cells were then incubated with D-luciferin (Gold Biotechnology St. Louis, MO; LUCNA-1g) at 37°C and 5% CO2 for 1 h in a 24-well plate (200 µl/well). In the last 15 min of incubation, samples were treated with or without Dyngo-4a. Immediately before imaging, cells were treated with 200 µl imaging media only or imaging media with glucagon (1 µM) and placed into a 37°C heated light-proof chamber. Plates were then imaged every 10 s for 20 min. Images were acquired using a 512 × 512 pixel electron multiplying CCD camera (Hamamatsu Photonics, Japan; C9100-13) using µManager 1.4. Analysis was completed using the multiple ROI analysis tool in the Fiji implementation of ImageJ. ROIs were drawn around each well, and corresponding background ROIs were placed in an area without cells. Intensity over time was measured and corrected for background luminescence for firefly luciferase values. A ratio of firefly to background luminescence was calculated per well over time. The max (average) of the top three proximal values of each treated condition was determined, and each condition was normalized to the max of the control sample.

RNA extraction and quantitative reverse transcriptase PCR

RNA was isolated from HEK293 cells using the QIAshredder and RNeasy Mini kit (Qiagen, 79654 and 74104, respectively). Briefly,

Gene	Primer sequences
GAPDH Human	F: 5′-CTGCCCAAGATCTTCCATGT-3′ R: 5′-GACAAGCTTCCCGTTCTCAG-3′
PCK1 Human	F: 5′-CTGCCCAAGATCTTCCATGT-3′ R: 5′-CAGCACCCTGGAGTTCTCTC-3′
SIK1 Human	F: 5′-GCTTCTGAACCATCCACACAT-3′ R: 5′-GTGCCCGTTGGAAGTCAAATA-3′
HPRT Mouse	F: 5′-TCAGTCAACGGGGGACATAAA-3′ R: 5′-GGGGCTGTACTGCTTAACCAG-3′
PCK1 Mouse	F: 5′-CTGCATAACGGTCTGGACTTC-3′ R: 5′-CAGCAACTGCCCGTACTCC-3′
G6PC Mouse	F: 5′-CTCTGGGTGGCAGTGGTCGG-3′ R: 5′-AGGACCCACCAATACGGGCGT-3′
PGC1α Mouse	F: 5′-ATGTGTCGCCTTCTTGCTCT-3′ R: 5′-CACGACCTGTGTCGAGAAAA-3′

TABLE 1: qRT-PCR primers.

after treatment, cells in a 6-well plate were placed on ice and washed once with cold PBS. Then cells were lysed, and RNA was extracted according to the manufacturer's protocol. RNA was eluted in RNAse free water, and the concentration of each sample was determined. cDNA was generated from RNA using iScript cDNA Synthesis Kit (Bio-Rad,1708891). Briefly, 1 µg of RNA was used per reaction primed with oligo dT. The reverse transcription reaction was performed according to the manufacturer's protocol.

qRT-PCR was performed using a StepOnePlus (Applied Biosystems, Foster City, CA) instrument. cDNA generated from extracted RNA was used as the input for the qRT-PCR, with amplification by Power SYBR Green PCR master mix (Applied Biosystems, 4367659). Transcript levels were normalized to GAPDH or HPRT. The primer pairs are listed in Table 1 above.

Statistical analysis and reproducibility

All data are shown as mean ± SD or SEM from at least three biologically independent experiments unless otherwise indicated. Images are representative of at least three biologically independent experiments. For primary hepatocyte experiments, three replicate plates were analyzed: two plates from one independent hepatocyte harvest and one plate from another independent hepatocyte harvest. Statistical analyses to determine significance were performed using Prism v.8 (GraphPad) for unpaired *t* test, one-way analysis of variance (ANOVA).

ACKNOWLEDGMENTS

These studies were supported by the U.S. National Institutes of Health (NIH; DA010711 and DA012864 to M.v.Z) and the UCSF Discovery Fund. E.L.S. was supported by the NIH IRACDA (K12 GM081266/GM/NIGMS at UCSF) and the CSU Program for Education & Research in Biotechnology (CSUPERB) New Investigator Award at SFSU. J.M.C. was supported by the San Francisco State NIH MBRS-RISE: R25-GM059298. E.H. was supported by Genentech Foundation Scholars program. We thank the members of the Sanchez Lab for their invaluable support and scientific discussions. We also thank the SFSU Cell and Molecular Imaging Center, and Genomics Transcriptomics Analysis Core, especially Annette Chan and Colleen Ingram. We also thank Nina Tsvetanova, Grace Peng, Nicole Fisher, Emily Blythe, Benjamin Barsi-Rhyne, and the other members of the von Zastrow lab for valuable advice and discussion. Finally, we thank DeLaine Larsen and Kari Herrington (Nikon Imaging Center, UCSF, NIH 1S10OD017993-01A1) for technical support and expertise as well as Jaquelyn J. Maher and Chris L. Her (UCSF Liver Center) for technical support and expertise in isolating primary mouse hepatocytes for these studies.

REFERENCES

Bagger JI, Knop FK, Holst JJ, Vilsbøll T (2011). Glucagon antagonism as a potential therapeutic target in type 2 diabetes. Diabetes Obes Metab 13, 965–971.

Bouschet T, Martin S, Henley JM (2005). Receptor-activity-modifying proteins are required for forward trafficking of the calcium-sensing receptor to the plasma membrane. J Cell Sci 118(Pt 20), 4709–4720.

Calebiro D, Nikolaev VO, Gagliani MC, de Filippis T, Dees C, Tacchetti C, Persani L, Lohse MJ (2009). Persistent cAMP-signals triggered by internalized G-protein-coupled receptors. PLoS Biol 7, e1000172.

Campbell JE, Drucker DJ (2015). Islet α cells and glucagon—Critical regulators of energy homeostasis. Nat Rev Endocrinol 11, 329–338.

Cegla J, Jones BJ, Gardiner JV, Hodson DJ, Marjot T, McGlone ER, Tan TM, Bloom SR (2017). RAMP2 influences glucagon receptor pharmacology via trafficking and signaling. Endocrinology 158, 2680–2693.

Godbole A, Lyga S, Lohse MJ, Calebiro D (2017). Internalized TSH receptors en route to the TGN induce local Gs-protein signaling and gene transcription. Nat Commun 8, 443.

Harden TK, Cotton CU, Waldo GL, Lutton JK, Perkins JP (1980). Catecholamine-induced alteration in sedimentation behavior of membrane bound beta-adrenergic receptors. Science 210, 441–443.

Irannejad R, Tomshine JC, Tomshine JR, Chevalier M, Mahoney JP, Steyaert J, Rasmussen SGF, Sunahara RK, El-Samad H, Huang B, von Zastrow M (2013). Conformational biosensors reveal GPCR signalling from endosomes. Nature 495, 534–538.

Janah L, Kjeldsen S, Galsgaard KD, Winther-Sørensen M, Stojanovska E, Pedersen J, Knop FK, Holst JJ, Wewer Albrechtsen NJ (2019). Glucagon receptor signaling and glucagon resistance. Int J Mol Sci 20. https://doi.org/10.3390/ijms20133314

Krilov L, Nguyen A, Miyazaki T, Unson CG, Bouscarel B (2008). Glucagon receptor recycling: Role of carboxyl terminus, beta-arrestins, and cytoskeleton. Am J Physiol Cell Physiol 295, C1230–C1237.

Lyga S, Volpe S, Werthmann RC, Götz K, Sungkaworn T, Lohse MJ, Calebiro D (2016). Persistent cAMP signaling by internalized LH receptors in ovarian follicles. Endocrinology 157, 1613–1621.

McGlone ER, Manchanda Y, Jones B, Pickford P, Inoue A, Carling D, Bloom SR, Tan T, Tomas A (2021). Receptor activity-modifying protein 2 (RAMP2) alters glucagon receptor trafficking in hepatocytes with functional effects on receptor signalling. Mol Metab 53, 101296.

Merlen C, Fabrega S, Desbuquois B, Unson CG, Authier F (2006). Glucagon-mediated internalization of serine-phosphorylated glucagon receptor and Gsalpha in rat liver. FEBS Lett 580, 5697–5704.

Pavlos NJ, Friedman PA (2017). GPCR signaling and trafficking: the long and short of it. Trends Endocrinol Metab TEM 28, 213–226.

Peng GE, Pessino V, Huang B, von Zastrow M (2021). Spatial decoding of endosomal cAMP signals by a metastable cytoplasmic PKA network. Nat Chem Biol 17, 558–566.

Rosenbaum DM, Rasmussen SGF, Kobilka BK (2009). The structure and function of G-protein-coupled receptors. Nature 459, 356–363.

Stauffer W, Sheng H, Lim HN (2018). EzColocalization: An ImageJ plugin for visualizing and measuring colocalization in cells and organisms. Sci Rep 8, 15764.

Stoeber M, Jullié D, Lobingier BT, Laeremans T, Steyaert J, Schiller PW, Manglik A, von Zastrow M (2018). a genetically encoded biosensor reveals location bias of opioid drug action. Neuron 98, 963–976.e5.

Tsvetanova NG, Irannejad R, von Zastrow M (2015). G protein-coupled receptor (GPCR) signaling via heterotrimeric G proteins from endosomes. J Biol Chem 290, 6689–6696.

Tsvetanova NG, von Zastrow M (2014). Spatial encoding of cyclic AMP signaling specificity by GPCR endocytosis. Nat Chem Biol 10, 1061–1065.

Weston C, Lu J, Li N, Barkan K, Richards GO, Roberts DJ, Skerry TM, Poyner D, Pardamwar M, Reynolds CA, *et al.* (2015). Modulation of glucagon receptor pharmacology by receptor activity-modifying protein-2 (RAMP2). J Biol Chem 290, 23009–23022.

Zeigerer A, Bogorad RL, Sharma K, Gilleron J, Seifert S, Sales S, Berndt N, Bulik S, Marsico G, D'Souza RCJ, *et al.* (2015). Regulation of liver metabolism by the endosomal GTPase Rab5. Cell Rep 11, 884–892.